chen xi (Orcid ID: 0000-0003-2297-866X)

Effective Leaching of Argillaceous and Dolomitic Carbonate Rocks for Strontium Isotope Stratigraphy

Xi **Chen*** and Ying **Zhou**

Department of Earth Sciences, University College London, Gower Street, London, WC1E 6BT, UK

* Corresponding author. e-mail: helen.xi.chen.19@ucl.ac.uk

Abstract

Various methods have been developed to extract a primary seawater Sr isotope signal from carbonate rocks for strontium isotope stratigraphy. However, there is little consensus around the best method due to variable sample purity and mineralogy. For this study, we applied sequential leaching to a range of rock samples in order to explore strontium isotope leaching systematics of less favoured argillaceous and dolomitic limestone samples. Following an ammonium acetate (NH_4Ac) prewash that removed ~ 10% of the carbonate fraction, a subsequent dilute acetic acid leach (10–30% aliquot) was shown to extract the lowest, demonstrably least altered seawater $^{87}Sr/^{86}Sr$ isotope ratios, along with in most cases seawater-like rare earth element (REE) plus yttrium (Y) patterns with the highest Y/Ho ratios (mostly > 36). Subsequent dissolution steps exhibited significantly elevated $^{87}Sr/^{86}Sr$ isotope ratios, Rb/Sr, Al/Ca and Mg/Ca ratios, indicating greater contributions from aluminosilicates and dolomite in the leachates. The new dissolution method by comparison significantly increases the likelihood of obtaining primary seawater $^{87}Sr/^{86}Sr$ isotope ratios from argillaceous

and dolomitic limestones where the other established procedures failed. Broad application of this approach could improve the temporal resolution of the seawater Sr isotope curve, especially where high purity limestone samples are scarce.

The secular trend of seawater strontium isotope ratio ($^{87}Sr/^{86}Sr$) reflects variations in the relative contributions of continental versus mantle reservoirs to ocean composition (Spooner 1976, Veizer 1989). In the open ocean, the residence time of Sr is much longer than the ocean circulation time ($\sim 10^6$ vs. $\sim 10^3$ years, respectively), so Sr isotopes are believed to be homogeneously distributed in the open seawater at any given time (Broecker and Peng 1983, Elderfield 1986, Hodell et $al.$ 1990). Strontium isotope stratigraphy (SIS) has been widely used for chemostratigraphic correlation and relies on the observation that the $^{87}Sr/^{86}Sr$ ratio in the world's oceans has varied over time (Burke et $al.$1982, Elderfield 1986, McArthur 1994, Veizer et $al.$ 1999), dating by comparison with reference curves (McArthur et $al.$ 2012, 2020), tracing diagenetic processes and depositional environment (Kuznetsov et $al.$ 2010, Stüeken et $al.$ 2017), and testing hypotheses of tectonic, biological and climatic evolution on geological timescales (e.g., Halverson 2007, Shields 2007, Hawkesworth et $al.$ 2016, Cawood et $al.$ 2018).

SIS studies must rely on diagenetically well-preserved chemical precipitates of seawater and well-honed selective dissolution methods. Diagenetic processes tend to increase $^{87}Sr/^{86}Sr$ values when interstitial fluids are influenced by evolved K-bearing silicates (e.g., Shields and Veizer 2002, Fairchild *et al.* 2018), or decrease Sr isotope composition when diagenetic fluids are influenced by mafic components, hydrothermal fluids or pressure solution of older, underlying carbonate rocks (e.g., Miller *et al.* 2008, Brand *et al.* 2010, Satkoski *et al.* 2017, Cui *et al.* 2020). Unfortunately, the well preserved, low-Mg calcite fossils, widely used in Phanerozoic SIS studies, are not available in Precambrian rocks, and so fine-grained carbonate components (e.g., diagenetic calcite microspar cement; Zhou *et al*. 2020), bulk carbonate rocks (e.g., micrite; Bailey *et al.* 2000) or non-carbonate rocks such as barite (e.g., McCulloch 1994, Satkoski *et al*. 2016, Roerdink *et al*. 2022), gypsum or anhydrite (e.g., Kah *et al.* 2001) and francolite (Li *et al.* 2011) have all been used instead for this purpose. Apart from diagenetic alteration, the leaching of detrital aluminosilicate phases during sample preparation can also introduce unintended Sr contamination, which is either released by ion exchange during the initial leaching stage or aluminosilicate dissolution during the later leaching process (McArthur 1994, Bailey *et al*. 2000, Bellefroid *et al*. 2018). Clay contamination during sample preparation normally would lead to Sr isotopes much higher than expected (Bailey *et al.* 2000), may result in overcorrection for radioactive Rb decay (Shields and Veizer 2002), and can mask the original diagenetic trend in a suite of samples (Bellefroid *et al.* 2018). Therefore, when conducting SIS, it is crucial that Sr is isolated from targeted and least altered minerals without contamination from extraneous phases, which requires appropriate dissolution methods.

The dissolution methods used in SIS studies can be divided into three main types: single-step bulk leaching methods, two-step sequential leaching methods and multiple-step sequential leaching methods (see recent review by Chen *et al*. 2022 and references therein). The most commonly used and effective sequential leaching method uses dilute acetic acid to target a certain proportion of pure carbonate, following an initial pre-leach with ammonium acetate or acetic acid to remove exchangeable Rb and Sr, while aiming to leave at least 10% carbonate undissolved (Bailey *et al*. 2000). This method has been developed further and is now widely used to extract primary carbonate signals from different types of carbonate rocks, using various pre-leaching cut-offs. For example, Bailey *et al*. (2000), confirmed subsequently by Li *et al*. (2011), suggested dissolving 30–40% of the carbonate portion of a sample, before targeting the following 30–40% for isotope measurement. Liu *et al*. (2013) suggested to pre-leach up to 70–80% of a dolostone sample, targeting the next 10–20% for analysis. Finally, Li *et al*. (2020) suggested an acidic pre-leach to dissolve ~ 60% of the carbonate, before targeting the next ~ 20% for both limestone and dolostone samples, but with emphasis on sample purity > 75% and > 90% for limestone and dolostone, respectively.

From the above, it is evident that few of any studies have sought to improve Sr isotope leaching methods for low purity and/or partially dolomitised samples, despite the lack of high purity limestones and large data gaps in Precambrian successions (Shields and Veizer 2002, Chen *et al*. 2022). Moreover, without a clear definition/classification system for sample purity and sample types, the application thresholds between different methods remain ill defined, with little consensus as to the most appropriate method. Therefore, it is imperative to conduct a systematic

methodological study on the abundant but less favoured argillaceous (often referred to as 'dirty' or 'muddy') and/or dolomitic limestones, and also test different leaching cut-offs / methods for samples using clear purity and Mg/Ca classification.

The rare earth element (REE) plus yttrium (REY) compositions of marine carbonate rocks could reveal depositional environment, redox conditions and diagenetic alteration (e.g., Satkoski *et al.* 2017, Verdel *et al.* 2018), thus might help us to determine if the Sr isotope data record seawater signal. The typical seawater REY profile shows progressive enrichment in heavier REE (James *et al.* 1995), while REY carbonate systematics are relatively resistant to diagenetic exchange compared with Sr isotopes due to the high partition coefficients of REY between calcite and seawater and generally low REY concentrations in diagenetic fluids (Zhong and Mucci 1995, Webb and Kamber 2000). However, carbonate REY components are very sensitive to detrital contamination due to the much higher REY contents and distinctly different shale-normalised REE patterns in detrital minerals (e.g., Nothdurft *et al.* 2004). Such a high sensitivity for clay contamination is also expected for Sr isotopes, and so comparing the REY pattern and Sr isotope ratios of individual leaching steps could help to validate the leaching method, especially for low purity carbonate rocks (James *et al.* 1995). The relatively clean proportion of the argillaceous and dolomitic carbonates during leaching procedures might be expected to demonstrate the most pristine, 'marine' REY patterns and Sr isotope values.

Based on earlier studies, such as Chilingar (1957) and Zhou *et al.* (2020), we divided samples into four types according to their Mg/Ca mass ratios (g g^{-1}), which are limestone (LST, Mg/Ca < 0.025), slightly dolomitic limestone (SDL, 0.025 < Mg/Ca

< 0.25), highly dolomitic limestone (HDL, 0.25 < Mg/Ca < 0.6) and dolostone (DST, Mg/Ca > 0.6). We define sample purity < 80% as argillaceous/low purity samples, and sample purity > 80% as relatively pure samples. In this study, we mainly aim to (1) conduct a systematic evaluation of a ten-step leaching procedure focusing mainly on argillaceous and dolomitic limestones (sample purity < 80%, 0.025 < Mg/Ca < 0.6) and identify the corresponding leachate representing seawater by comparing measured $^{87}Sr/^{86}Sr$ isotope ratios of each step to contemporaneous seawater $^{87}Sr/^{86}Sr$ isotope signature; (2) use REY patterns to assist in the discussion of Sr isotope leaching results and explore the connections and differences between these two systems; (3) compare the applicability of leaching procedure from this study with established protocols using a sample set with various purities and Mg/Ca ratios from the Gaoyuzhuang Formation; and (4) propose new thresholds for sample screening in future SIS studies.

Geological setting and sample descriptions

Geological background

The ~ 1.65–1.4 Ga Jixian Group consists of five Formations (Gaoyuzhuang, Yangzhuang, Wumishan, Hongshuizhuang and Tieling in ascending order), which represent near-continuous marine deposition within the Yanliao Basin, North China Craton. The ~ 1.6–1.55 Ga Gaoyuzhuang Formation is further divided into four lithological members in ascending order: Guandi Member (M1), Sangshu'an Member (M2), Zhangjiayu Member (M3) and Huanxiusi Member (M4). Most samples in this study were collected from the ~ 1.57–1.56 Ga Zhangjiayu Member (M3) (Li *et al.* 2010, Tian *et al.* 2015), through an interval that covers a negative carbon isotope

excursion (Li *et al*. 2003, Guo *et al*. 2013, Zhang *et al*. 2018). The Zhangjiayu Member consists mainly of limestone and dolomitic limestone deposited in the shallow marine environment, with argillaceous and variably dolomitised limestone and black shale mainly in the lower part, showing a shallowing-upward cycle (e.g., Mei *et al.* 2005, Zhang *et al.* 2018). The impure, dolomitic limestones of Zhangjiayu Member provide a good opportunity for us to examine the leaching method for this type of rock. Based on a new compilation of the Precambrian seawater Sr isotope curve (Chen *et al.* 2022), the published and screened seawater $^{87}Sr/^{86}Sr$ data between 1.60 Ga and 1.55 Ga range from ~ 0.7046 to ~ 0.7056 (e.g., Ray *et al*. 2003, Kuznetsov *et al*. 2008, Bellefroid *et al*. 2018, Tan *et al*. 2020), which are compared with data obtained in this study.

Samples

Samples of varying purity and dolomitisation were collected from the Zhangjiayu Member (M3) at Jixian (J), Pingquan (P), Gangou (G), Kuancheng (K), Huanxiusi (HXSZ) and Sangshu'an (SSAZ) sections, and underlying Huanxiusi Member (M4, abbreviated to HXS) on the North China Craton. Samples analysed in this study were micro-drilled to extract powder to avoid visibly secondary portions such as cross-cutting veins, late-stage void filling spar and dissolution features etc. After that, powders of each sample were dissolved in HNO_3 (w (HNO_3) = 2%) for bulk carbonate major and trace elements before undergoing leaching steps. Stable isotopes ($\delta^{13}C_{VPDB}$ and $\delta^{18}O_{VPDB}$) were also analysed to help with sample selection and diagenetic screening. Five samples (J95, G99, K46, G90 and HXSZ4) from four different sections (Jixian, Gangou, Kuancheng and Huanxiusi) of Zhangjiayu Member (M3) were selected to develop a leaching method for argillaceous and dolomitic

limestone. These samples have Mg/Ca ratios ranging from ~ 0.06 to 0.4 g g^{-1} with carbonate contents ranging from 50% to 75%, and with few obvious signs of significant diagenetic alteration (for example, in most cases Mn/Sr < 1 g g^{-1}, $\delta^{13}C_{VPDB}$ close to ~ 0, $\delta^{18}O_{VPDB}$ at -3 ~ -6‰). The five samples were used for sequential leaching experiments alongside rock reference material LS19 (a pure limestone from the Huaibei Group, Mg/Ca = 0.02 g g^{-1}) from Zhou *et al.* (2020) with a published Sr isotope value of 0.705439 ± 0.000008 (2s, N = 13); and one reference material CRM 88a (a pure dolostone, Mg/Ca = 0.6 g g^{-1}) with a published Sr isotope value of 0.71022 ± 0.00004 (2s, N = 4) (Stammeier *et al.* 2020). The detailed bulk rock information for all samples used for this study is summarised in **Table 1**. Another twenty samples with various sample purities and Mg/Ca ratios were studied to examine the leaching methods, the bulk carbonate information of which is reported alongside Sr isotope result in **Table 4**.

< Table 1 here >

Methods

Sample preparation method

Bulk carbonate dissolution: For preparation of bulk carbonate major and trace element measurement, sample powder (~ 10–20 mg) was dissolved in 5 ml of HNO_3 (w (HNO_3) = 2%) for 24 h, then centrifuged at 3600 rpm, for 5 min. The supernatant was collected and diluted with HNO_3 (w (HNO_3) = 2%) for elemental determination.

Ten-step sequential leaching procedure: Micro-drilled sample powder was ground by hand using an agate pestle and mortar to avoid coarse flakes, and then around 100–200 mg of each sample was transferred to 10 ml centrifuge tubes to carry out the sequential leaching procedure. Modified after Bailey *et al.* (2000), a ten-step leaching procedure was applied to argillaceous, dolomitic limestones (J95, G99, K46, G90, HXSZ4) and CRM 88a, while a six-step leaching procedure was applied to pure limestone LS19. All samples were prewashed with 1 mol l^{-1} ammonium acetate, followed by dilute acetic acid (0.05–0.5 mol l^{-1}) dissolution. In each step, based on total carbonate content, the acid volumes were designed to dissolve ~ 10% carbonate for argillaceous and dolomitic limestones and CRM 88a, and ~ 20% for pure limestone LS19. After the acid was added, samples were ultrasonically agitated (0.5–2 h) and allowed to stand for 0.5–2 h at 25–40 °C, then were centrifuged at 3600 rpm for 5 min. The supernatant was collected for Sr isotope and elemental determination, and the residue washed with ultrapure water one time before the next leaching step. The carbonate proportion being leached out in each step was calculated by using mass of ($CaCO_3$ + $MgCO_3$) in each leaching step divided by mass of ($CaCO_3$ + $MgCO_3$) in the whole sample. In total, more than 95% of carbonate was dissolved from each sample. Detailed leaching protocol is summarised in **Table 2.**

< Table 2 here >

Leaching methods' comparison: Twenty samples with various sample purities and Mg/Ca from 0 to 0.6 g g^{-1} (i.e., limestone, slightly and highly dolomitic limestone) from the Gaoyuzhuang Formation were selected to examine the suitability of various leaching cut-offs for different types of rocks (note: samples with Mg/Ca >

0.6 g g^{-1} are not examined in this study). The following leaching methods are compared: method 1 – prewash using ammonium acetate, then target the first 10–30% (this study); method 2 – pre-leach 30–40%, then target the next 30–40% (Bailey *et al.* 2000, Li *et al.* 2011); method 3 – pre-leach 60–70%, then target the next ~ 20% (Liu *et al.* 2013, Li *et al.* 2020). We conducted a four-step leaching experiment (simplified from the ten-step leaching method above), which was designed to dissolve ~ 30% carbonate in each step after a 1 mol l^{-1} ammonium acetate prewash. Accordingly, the leachates from steps 1, 2 and 3 roughly correspond to cut-offs in methods 1, 2 and 3 respectively, which were then measured for Sr isotopes.

Analytical method

　　Elemental determination: Elemental determinations, including major, trace and rare earth elements (REE) plus yttrium (Y), were carried out in the Cross-Faculty Elemental Analysis Facility, University College London (UCL), for solutions of bulk carbonate and all leaching supernatants of selected samples and rock reference materials. Major element mass fractions (including Ca, Mg, K, Na, Fe, Mn, Al and Sr) in carbonate leachate were measured by inductively coupled plasma-atomic emission spectrometry (Varian 720 ICP-AES). The calibration curve was generated by serial dilution of multi-element stock solution (Superco, Sigma-Aldrich). Each data point is the mean of six replicates, with the RSD being < 3% in all the determined elements. Trace element Rb, Y and rare earth element (REE) concentrations of carbonate leachates were measured by inductively coupled plasma-mass spectrometry (Agilent 7900 ICP-MS) and run against multi-element matrix-matched standards (Superco, Sigma-Aldrich) within an appropriate concentration range. Each data point is the mean of seven replicates, with the RSD being < 5% in all the determined elements.

Sr, C and O isotope measurement: For Sr isotope measurement, small polypropylene columns with polypropylene frits (~ 30 μm) and ~ 1 cm thickness of Eichrom® Sr specific resin were used for Sr separation in an ISO 7 (Class 10000) geochemistry laboratory at UCL. The supernatant in each leaching step (prepared according to methods in sections *Ten-step sequential leaching procedure* and *Leaching methods' comparison*) was dried in PTFE beakers on a hot plate before being dissolved in 0.5 ml 4 mol l^{-1} nitric acid and then passed through the pre-cleaned and conditioned columns. The column was sequentially eluted with 1ml of 8 mol l^{-1} of HNO$_3$, and twice with a full reservoir of 8 mol l^{-1} HNO$_3$ to primarily wash out the matrix. Afterwards, two full reservoirs of high-purity (Milli-Q) water were used to elute Sr. The collected eluant was then dried and redissolved in HNO$_3$ (w (HNO$_3$) = 2%) for conventional ^{87}Sr/^{86}Sr isotope measurement. The ^{87}Sr/^{86}Sr isotope ratios were measured using a Nu Instruments Plasma 3 multi-collector inductively coupled plasma mass spectrometer (MC-ICP-MS) at UCL. Instrumental isotopic fractionation (IIF) was corrected using the exponential law (to ^{86}Sr/^{88}Sr = 0.1194), followed by a standard bracketing method. The interferences of ^{87}Rb were corrected using an ^{87}Rb/^{85}Rb ratio of 0.3857. The interferences of Kr were corrected by a blank measurement before each sample. Reported (conventional) ^{87}Sr/^{86}Sr ratios were corrected to the published value (0.710252 ± 0.000013; Weis *et al.* 2006). The repeatability was reported both as the "internal" standard error (2SE) for each sample and standard deviation (2*s*) for repeated measurements of NBS 987 in each session, see **Table 3 and 4**. An in-house carbonate reference material (N1, modern shell) was processed along with sample leachates and its multi-run mean (with intermediate precision) was 0.70918 ± 0.000018 (2*s*, $N = 10$), which is comparable to the modern

seawater value (0.709175 ± 0.0000012; Kuznetsov *et al.* 2012). A procedural blank was included in each batch of samples with Sr quantities below 0.1 ng representing less than 0.01% contribution to the samples' (Sr quantities ~ 1 µg) measurement results.

For C and O isotope measurement, powdered carbonate was analysed at the Bloomsbury Environmental Isotope Facility (BEIF) at University College London on a continuous-flow (ThermoFisher Delta V) mass spectrometer linked to a Gas Bench II device. The repeatability ($2s$, $N = 3$) from reference materials (NBS 19) was better than ± 0.08‰ for $\delta^{13}C$ and ± 0.1‰ for $\delta^{18}O$. All values are reported using the Vienna Pee Dee Belemnite notation (VPDB) relative to NBS19 ($\delta^{13}C_{VPDB} = 1.95‰$, $\delta^{18}O_{VPDB} = -2.2‰$).

Results

Step leaching Sr isotopic and elemental variation

$^{87}Sr/^{86}Sr$ isotope ratios and elemental (Mg/Ca, Mn/Sr, Sr/Ca, Rb/Sr, Ba/Ca, K/Ca, Al/Ca, Fe/Ca) ratios, and cumulative percentage carbonate dissolution for all leaching steps for samples (J95, G99, K46, G90, HXSZ4) and two rock reference materials (LS19, 88a) are shown in **Table 3** and **Figure 1.**

For all types of rocks, $^{87}Sr/^{86}Sr$ isotope ratios in step 0 (1 mol l^{-1} NH$_4$AC prewash) show very high (or the highest) values. The pure limestone sample (LS19) exhibits lowest Sr isotope ratios in all three middle leachates (S1–S3), corresponding to the middle ~ 5–70% carbonate dissolution, before rising in the final two leaching steps.

The lowest Sr isotope values in S1–S3 are associated with lower Mg/Ca, Mn/Sr, Rb/Sr, K/Ca, Ba/Ca, Al/Ca, Fe/Ca ratios, and a higher Sr/Ca ratio than both the prewash and the last two leachates. The middle three values of LS19 measured in this study (0.70543 ± 0.00003; $2s$, $N = 72$) are consistent with what has been reported (0.705439 ± 0.000008; $2s$, $N = 13$) by Zhou *et al.* (2020) within error.

Sequential dissolution of argillaceous and dolomitic limestone (SDL and HDL), following the NH4Ac prewash, results in a lowest $^{87}Sr/^{86}Sr$ isotope value in S1 (~ 10–30% carbonate dissolution), an increase in S2 and a dramatic increase in the last two steps. The lowermost Sr isotope ratios of argillaceous and dolomitic samples range from 0.70503 to 0.70533, similar to the reported seawater range during 1.60–1.55 Ga (0.7046–0.7056; e.g., Ray *et al.* 2003, Kuznetsov *et al.* 2008, Bellefroid *et al.* 2018, Tan *et al.* 2020). In general, Sr isotope ratios are higher when elemental ratio indicators of alteration, such as Mg/Ca, Rb/Sr, Ba/Ca and K/Ca, are higher. From S1 onwards, Sr/Ca shows a gradually decreasing trend, while Mn/Sr shows an increasing trend. Al/Ca and Fe/Ca ratios rise more clearly only after S6.

The $^{87}Sr/^{86}Sr$ isotope values of the pure dolostone sample (88a) have two apparent dips at S1-S2 and S7-S8, which correspond to 20–30% and 70–80% of carbonate dissolution, respectively, with the lowest value found in S7-S8 (0.710043) **(Figure 1D)**. Mg/Ca increases gradually from S0 to S9. Mn/Sr, Sr/Ca, Rb/Sr, Ba/Ca and K/Ca ratios decrease after S0 and remain stable since S1, which are mirrored by Al/Ca, Fe/Ca ratios.

< Figure 1 here >

< Table 3 here >

Step leaching REY pattern

To help understand the leaching pattern of Sr isotopes for argillaceous and dolomitic limestones, we also examined their step-leaching REY pattern **(Figure 2, Table S2)**. The stepwise REY mass fraction is calculated based on the mass of Ca, Mg carbonate being leached out (i.e., mass of REY divided by mass of $CaCO_3 + MgCO_3$ in each step). All REY mass fractions were normalised to post-Archaean Australian Shale (PAAS: Pourmand *et al*. 2012). Supernatants of ammonium acetate prewash exhibit a non-seawater pattern, either being flat or displaying a positive Eu anomaly. Ba/Sm ratios show a strong correlation with $Eu_{sn}/Eu*_{sn}$ for all argillaceous and dolomitic limestones, strongly implying that Eu anomalies in the S0 resulted from BaO interference in the ICP-MS (Jarvis *et al.* 1989), while no such correlation was observed for other leaching steps **(Figure S1)**. A seawater-like REY pattern occurs in S1 for almost all samples but tends to be flat in the subsequent leaching steps. The only exception is G99, which shows a non-seawater pattern and a negative Eu anomaly throughout all leaching steps. The Y/Ho ratios of the argillaceous and dolomitic limestone in each leaching step are shown in **Figure 3.** All samples display a Y/Ho ratio > 36 in S1, and then the ratio gradually decreases in subsequent steps.

< Figure 2 here >

< Figure 3 here >

Leaching methods' comparison results

As mentioned before (section *Leaching methods' comparison*), twenty carbonate samples with various purity are selected to test the three different leaching methods: Method 1 (this study) – target the first 10–30% after NH_4Ac prewash; Method 2 – pre-leach 30%, target the next 30%, developed mainly for high purity limestone (Bailey *et al.* 2000, Li *et al.* 2011); Method 3 – pre-leach 60–70%, target the next ~ 20%, developed for dolostone (Liu *et al.* 2013, Li *et al.* 2020). Strontium isotope results and bulk carbonate information for each sample are shown in **Table 4** and **Figure 4.** For pure limestone (HXS1), no significant differences are evident between the three different leaching cut-offs (i.e., the disparities are within measurement errors). For some very argillaceous samples (carbonate content $\leq \sim 50\%$) such as G94 and G97, applying higher leaching cut-offs (i.e., methods 2 and 3) would increase the Sr isotope ratios dramatically (up to 0.009 compared with targeting the first 10–30% after prewash). Relatively pure dolomitic limestones (carbonate percentage > 80% and $0.025 < Mg/Ca < 0.6$ g g^{-1}) such as K68, K66, K73.5, P60, K49, K65 also tend to reach the lowest values using method 1, the method this study recommends, although adjusting cut off points would not produce the more extreme differences seen in very argillaceous samples. When $Mg/Ca > 0.4$ g g^{-1}, $Mn/Sr > 2$ g g^{-1} or $Sr/(Ca+Mg) < 200$ µg g^{-1} the situation becomes quite complicated, i.e., the lowest value could be generated by any of the leaching methods, but no near-seawater values are observed.

< Figure 4 here >

< Table 4 here >

Discussion

Explanations of step-leaching Sr isotope and elemental variations

The leaching step showing the lowest, and likely most pristine Sr isotope ratios may correspond to the effective isolation of either the clay-free carbonate fraction and/or the least altered carbonate phase in a given sample. Rubidium, K and Al mass fractions are typical indicators of aluminosilicate Sr contamination (Banner *et al*. 1988, McArthur 1994, Montañez *et al*.1996). Rubidium and K can both be used to track clay surface-bound Sr released by ion exchange as well as detrital / authigenic clay dissolution. By contrast, Al might not be a suitable proxy for Sr released from clay surfaces due to its insoluble nature (Bellefroid *et al.* 2018), but it is a strong sign of aluminosilicate dissolution (Wierzbowski *et al.* 2012). Mg/Ca is used to quantify the relative contribution of calcite and dolomite during leaching steps and the degree of dolomitisation in a sample. Mn/Sr, Fe/Ca and Sr/Ca are often used as indices of alteration, and Mn/Sr, Fe/Ca are generally expected to be higher, while Sr/Ca is considered to be lower in diagenetically altered samples than in coeval seawater (Banner and Hanson 1990, Gorokhov *et al*. 1995, Kaufman and Knoll 1995). This general relationship is complicated by variable redox conditions, diagenetic fluids and mineralogy. For instance, compared with calcite, dolomite generally has a greater preference for Fe and Mn (Mazzullo 1992) and a lower preference for Sr (Vahrenkamp and Swart 1990). Apart from diagenetic phases, the stepwise leaching patterns of Mn/Sr and Fe/Ca might also indicate the dissolution of non-carbonate phases such as Fe-Mn oxides (e.g., Zhang *et al*. 2015).

Argillaceous and dolomitic limestones:

- Similarities among samples. All argillaceous and dolomitic limestones exhibit a similar Sr isotope leaching pattern, i.e., reaching a nadir in S1, and then rising through subsequent steps. A comparable pattern was previously reported by Bellefroid *et al.* (2018) on limestones of the Dhaiqa and Tieling Formations, where it was referred to as a "V"-shaped pattern. The extremely radiogenic Sr and high Rb/Sr, K/Ca ratios of the first leaching step (S0) by ammonium acetate are contributed to significantly by Sr in ion exchange sites in clay minerals and trace metals adsorbed on mineral surfaces (Morton 1985, Gao 1990, Bailey *et al.* 2000). The dramatic drop of Rb/Sr, K/Ca and $^{87}Sr/^{86}Sr$ isotope ratios in the following step (S1, in some cases S2) indicates that pre-cleaning has effectively removed this weakly surface-bound Sr. The increase in Rb/Sr, K/Ca and Al/Ca ratios and more radiogenic $^{87}Sr/^{86}Sr$ isotope ratios from S2, and especially after S6, most likely implies partial dissolution of residual aluminosilicate, considering the samples' argillaceous lithology. Non-carbonate component increases proportionally as carbonate dissolves. As the volume of acid was greater and reaction time was longer, a larger amount of non-carbonate fraction was dissolved, leading to a dramatic increase in $^{87}Sr/^{86}Sr$ isotope ratio. Intriguingly, we found that Ba/Ca follows a similar pattern and exhibits a strong linear correlation with Rb/Sr ($R^2 > 0.95$; Figure S2). Previous research found that clay is one of the main Ba-carriers in marine sediments (Rutten and de Lange 2002, Gonneea and Paytan 2006). Therefore, the strong correlation between Rb and Ba might support the use of Ba/Ca ratios as indicators of clay contamination. Low Mg/Ca ratios (all below 0.1 g g^{-1}) in S1 for all argillaceous and dolomitic limestones indicate that the calcite proportion was leached out before dolomite as calcite reacts much faster with

acid than dolomite. Gradually increasing Mg/Ca, Mn/Sr and Fe/Ca and decreasing Sr/Ca after S1 demonstrate that the calcite proportion in S1 is the closest to primary carbonate phase, which is released before secondary calcite, dolomite and non-carbonate minerals are dissolved in subsequent leaching steps.

- Disparities among samples. Slight differences still exist among samples (J95, G99, G90, K46, HXSZ4), and more explanations could be investigated by cross plotting the stepwise elemental ratios (Rb/Sr, Mn/Sr and Mg/Ca) against Sr isotopes **(Figure 5)**. After reaching the minimal value in S1, J95, a slightly dolomitic limestone, shows a slower rebound to a higher value compared with other samples. The step leach Rb/Sr, Mn/Sr and Mg/Ca ratios of J95 show the weakest relationship with Sr isotopes (from S2 to S9) compared with other samples, which indicates that clay contamination and leaching of diagenetic phases did not influence the Sr isotope values immediately from S2 **(Figure 5, A1-A3)**. With a Mg/Ca ratio (0.06 g g^{-1}) close to limestone (< 0.025 g g^{-1}), and a carbonate content of ~ 70%, J95 contains a relatively higher proportion of "clean and primary" calcite compared with the other four argillaceous and dolomitic limestones (G99, K46, G90, HXSZ4). In contrast, all samples except J95 show positive correlations between Rb/Sr and ^{87}Sr/^{86}Sr isotope ratios **(Figure 5, B1-E1)**, whereby the 'dirtiest' sample (G99) has the strongest correlation (R^2 = 0.91, **Figure 5, B1**). This result demonstrates that for very argillaceous samples, the Sr isotope leaching pattern is strongly and rapidly influenced by the dissolution of clay minerals, immediately following the first leachate, even when using a weak acid.

Therefore, caution needs to be taken to avoid over-leaching when dealing with argillaceous samples, while the first 10–30% after prewash would seem to represent the cleanest portion. One possible factor that influences clay mineral dissolution could be reaction time. The longer agitation in the ultrasonic bath and reaction time since S3 **(Table 2)** could have contributed to the dissolution of more clay minerals. This may indicate that when leaching dirty/muddy samples for Sr isotope measurement, shorter reaction time is preferable. Cross-plots of stepwise Mg/Ca and Mn/Sr versus Sr isotope ratios (**Figure 5, A2-E2, A3-E3**) in most cases exhibit a stronger covariation in highly dolomitic limestone (G90, HXSZ4) than for slightly dolomitic limestones (J95, G99, K46), which possibly indicates that dissolution of the dolomitised (likely more diagenetically altered) proportion is a more important contributing factor that leads to increased $^{87}Sr/^{86}Sr$ isotope ratios after S1 for samples with a higher degree of dolomitisation.

< Figure 5 here >

Two rock reference materials: Although a detailed discussion on SIS leaching methods for pure limestone and dolostone samples is beyond the scope of this study, we wish to show how different types of rocks behave by briefly demonstrating the leaching patterns of two rock reference materials here. In pure limestone in-house reference material LS19, the "clean and primary" proportion is much higher than in argillaceous and dolomitic limestones, as evidenced by a consistent Sr isotope nadir alongside the lowest Mg/Ca and Mn/Sr ratios from S1 to S3, which corresponds to ~ 5% to 70% carbonate dissolution. This pattern is

consistent with previous studies on limestone samples (e.g., Bailey *et al*. 2000, Bellefroid *et al*. 2018). Interestingly, the $^{87}Sr/^{86}Sr$ isotope ratio leaching pattern for CRM 88a exhibits two low points in steps S1/S2 and S7/S8, respectively, although none of these show seawater values as both sets of values are considerably higher than contemporaneous seawater. Therefore, the leachates of CRM 88a might contain calcite and dolomite formed at different stages of recrystallisation. Nevertheless, the lowest $^{87}Sr/^{86}Sr$ isotope value of 88a from this study is significantly lower than reported by Stammeier *et al*. (2020), in which the bulk sample was dissolved in 3 mol l^{-1} HNO$_3$.

Comparison of $^{87}Sr/^{86}Sr$ isotope ratios with REY step-leaching pattern

Clay contamination: The high sensitivity to clay contamination of both REY patterns and Sr isotopes allows us to combine them to examine the validity of the leaching method for argillaceous and dolomitic limestones. The step leaching REY patterns of all samples, except for G99, show a seawater pattern in S1 (and some in S2), which is in line with Sr isotope leaching patterns (lowest/seawater $^{87}Sr/^{86}Sr$ isotope ratios in S1). This result is also consistent with previous studies such as Tostevin *et al*. (2016) and Cao *et al*. (2020), which proposed that the early leaches contain more pristine seawater REY signals for partially dolomitised and less pure limestones. The Y/Ho ratio is one of the most effective approaches to recognising terrigenous influences on seawater REY distribution because Ho is scavenged two times faster than Y from the surface ocean to the deep ocean (Nozaki *et al*. 1997). The Y/Ho ratio of seawater is consequently almost twice that of the mean upper continental crust (~ 26–28; Taylor and McLennan 1981, Kamber *et al*. 2005). Y/Ho > 36 is a commonly used threshold value for seawater REY signals (e.g., Tostevin *et al*.

2016). The high Y/Ho ratios of S1 (> 36, **Figure 3**), before gradually decreasing in subsequent steps, further confirms our findings based on Sr isotopes, i.e., that step 1 leaches out the most primary portion of the sample. A conflicting story (i.e., a decreasing $^{87}Sr/^{86}Sr$ accompanied by a decreasing Y/Ho) was reported by Verdel *et al.* (2018), in which the authors attribute the disparity to the progressive dissolution of different combinations of sources. Nevertheless, the high consistency between REY compositions and Sr isotope leaching pattern in this study further confirmed a similar sensitivity of both systems to clay contamination.

Organic matter activity and dolomitisation: Even though the REY pattern is consistent with the Sr isotope leaching pattern in most samples, an exception still exists in G99, the sample with a seawater like Sr isotope value but without a seawater REY pattern. One difference between G99 and other samples is that G99 contains high levels of organic compounds (total TOC of 1.3%). It seems probable to us that during early diagenesis, degradation and remineralisation of organic matter released adsorbed REY into pore waters so it could be incorporated into carbonate rocks, altering the original seawater REY pattern. The potential for substantial, indirect influence from organic degradation on the original carbonate REY pattern was also proposed in a recent study by Zhang and Shields (2022). Some research shows that organic matter preferentially absorbs LREE and then releases it at depth during remineralisation (Chen *et al.* 2015, Meyer *et al.* 2021), but the understanding of REY in the biological system is still at an early stage; thus, a range of REY patterns in organic matter might be expected (Zhang and Shields 2022). In contrast to REY patterns, the low Sr content of organic matter means that it will have little influence on pore fluid Sr isotope composition.

In addition, the highly dolomitic limestones (G90, HXSZ4) also show marine-like REY patterns in S1. This finding is consistent with the previously proposed argument that dolomitisation may not significantly alter REY patterns of carbonate rocks (Banner *et al*. 1988, Zhang *et al*. 2015), although it might change Sr isotope characteristics. Therefore, while REY and Sr isotopes in carbonates have similarities (e.g., both are vulnerable to clay contamination), other factors (e.g., organic matter, dolomitisation) will have different impacts on these two systems.

Effectiveness of ammonium acetate prewash: Ammonium acetate prewash has been widely used for leaching protocols of carbonate rocks for different proxies such as REY, Sr isotopes or Li isotopes to remove the ion-exchangeable phase (Tessier *et al*. 1979, Bailey *et al*. 2000, Kuznetsov *et al*. 2010, Liu *et al*. 2013, Pogge von Strandmann *et al*. 2013, Cui *et al*. 2015, Bellefroid *et al*. 2018, Cao *et al*. 2020). It was suggested that using dilute acetic acid may remove Sr contamination more effectively (Bailey *et al*. 2000), but based on our study for the argillaceous and dolomitic limestones, using higher volumes of acetic acid or longer reaction time might cause the prewash to leach out far more carbonate than the targeted ~ 5%. Instead, this problem is easily solved by using *p*H neutral ammonium acetate.

We agree that ammonium acetate might not remove all clay surface-bound contamination (e.g., Bailey *et al.* 2000), but based on major and trace element, REY and Sr isotope data (as discussed in previous sections), using an ammonium acetate prewash is still an effective option. It is also worth noting that the reaction time may play a significant role in the effectiveness of using ammonium acetate. It was

suggested that a 30-minute leaching time is sufficient to achieve maximum extraction of adsorbed REE (Moldoveanu and Papangelakis 2013, Cao *et al.* 2020) and this reaction time was also applied in this study.

Suitability of different leaching cut-offs for different types of samples

The pure limestone (HXS1) shows no significant difference between the three different leaching cut-offs (**Figure 4 and Table 4**), which is consistent with the leaching pattern of pure limestone LS19 (**Figure 1, C1**). However, for very argillaceous samples (% carbonate $\leq \sim 50\%$) with Mg/Ca < 0.4 g g^{-1}, such as G94, G97, applying any higher pre-leach cut-offs would produce a sizeable error compared with using the first 10–30% after prewash, similar to what we show for the leaching pattern of G99 (**Figure 1, A1**). This is because to extract the primary signal from carbonate rocks, two requirements must be met simultaneously: "relatively clay-free" and "least altered", and the only possible proportion for argillaceous and dolomitic limestones is the first 10–30%, which would be readily missed if samples are over-leached during pre-leach. By contrast, the different leaching cut-offs for pure samples (carbonate content > 80%) with Mg/Ca < 0.4 g g^{-1} (e.g., K66, K73.5, **Figure 4**) do not produce as large a difference as the more argillaceous samples. In general, most samples with Mg/Ca < 0.4 g g^{-1} yield the lowest/seawater Sr isotopic values with the first $\sim 30\%$ dissolution after prewash (**Figure 4, Table 4**), which implies that for most of the limestones and slightly dolomitic limestone samples of the Gaoyuzhuang Formation, the calcite proportion dissolved in the early stage contains the primary marine signal. It is worth noting that samples G114, G151 and G176, despite having Mg/Ca values below 0.4 g g^{-1}, could not produce seawater values using any of the three methods. Higher Mn/Sr ratios (> 2 g g^{-1}) for G114 and G151 and lower

Sr/Ca+Mg (< 200 µg g^{-1}) for G176 suggest possibly higher level of diagenetic alteration and thus modification of the original seawater signal in the carbonate. When Mg/Ca > 0.4 g g^{-1}, it is unpredictable which method will yield the lowest ^{87}Sr/^{86}Sr isotope ratio , and all lowest values are higher than the proposed seawater value (**Figure 4**). One possible contributing factor is leaching out other calcite components, in the form of dedolomitisation or secondary veins and cements, especially in highly dolomitic limestones and dolostones (e.g., Tostevin *et al*. 2016).

By comparison, targeting the first ~ 10–30% carbonate after ammonium acetate prewash appears to be the most appropriate method for SIS using a wide range of carbonate, especially argillaceous and dolomitic limestones (recommended protocol from this study summarised in **Figure 6**) with detailed thresholds described in section *Recommended cut-offs for sample screening in SIS studies*. The widely used cut-off for bulk carbonate (with 30% pre-leach) is more suitable for limestones or pure dolomitic limestones than for other rock types. Although our study and Liu *et al*. (2013, 2014) show pre-leaching of 60–70% can obtain the lowest ^{87}Sr/^{86}Sr isotope ratio for highly dolomitic limestones or dolostones, our data present that the lowest Sr isotopic value of CRM 88a (Mg/Ca = 0.6 g g^{-1}) and other samples with Mg/Ca > 0.4 g g^{-1} are higher than contemporaneous seawater, therefore, without further tests, no recommendations can be made for these types of samples.

< Figure 6 here >

Recommended cut-offs for sample screening in SIS studies

Based on our leaching tests and the application of three different methods to twenty samples with different sample purity and dolomitisation, we noticed that samples with either Mg/Ca > 0.4 g g^{-1} and Mn/Sr > 2 g g^{-1} or [Sr] < 200 µg g^{-1} would be less likely to retain the original seawater signal (i.e., all the lowest ^{87}Sr/^{86}Sr isotope ratios from these types of samples yielded from three leaching methods are higher than contemporaneous seawater values). Cross-plots of Sr isotopes (lowest values among three methods) versus bulk Mg/Ca, Mn/Sr, % carbonate and Sr/(Ca+Mg) **(Figure 7)** further illustrate that when Mg/Ca < 0.25 g g^{-1}, [Sr] > 400 µg g^{-1}, Mn/Sr < 2 g g^{-1}, the success rate (the likelihood to obtain seawater value) will be high. A previous study by Li *et al*. (2020) suggested that samples with high purities (> 75% for limestones, > 90% for dolostones) are more suitable for SIS. Even though sample purity influences the likelihood of obtaining seawater values if the proposed seawater Sr isotopic ratio range is valid, our data (**Figure 4a, Figure 7d**) show that our leaching method increases that likelihood significantly, in four out of six cases with carbonate content < 70% when other thresholds are met.

Our suggested thresholds here are based on the lowermost value among three leaching methods for the twenty selected samples from the Gaoyuzhuang Formation. The thresholds proposed from this study are in agreement broadly with previously proposed thresholds by different studies (e.g., Bartley *et al*. 2001, Halverson *et al*. 2007, Bold *et al*. 2016, Cox *et al*. 2016, Gibson *et al*. 2019, Zhou *et al*. 2020). We agree that it is unlikely to have any single criterion for the robust screening of altered samples because the post-depositional history varies from basin to basin (Bartley *et al*. 2001, Melezhik *et al*. 2001, Halverson *et al*. 2007), but the consistency between

different research might provide a valuable reference for future Precambrian SIS studies.

< Figure 7 here >

Conclusions

The major conclusions of this study are summarised below:

(1) A Sr isotope leaching method for argillaceous and dolomitic limestones has been developed, whereby the most effective approach involves extracting the first 10–30% carbonate using weak acetic acid after ammonium acetate prewash.

(2) REY patterns of carbonate rocks, in agreement with Sr isotopes, exhibit the most seawater-like patterns in the first leach after NH4Ac prewash.

(3) Organic matter remineralisation during early diagenesis might influence the REY patterns of carbonate rocks but will not have much influence on Sr isotopes, while Sr isotopes are more vulnerable to dolomitisation compared with REY. Both $^{87}Sr/^{86}Sr$ isotope ratios and REY in carbonates are sensitive to clay contamination.

(4) The developed method could identify pristine $^{87}Sr/^{86}Sr$ isotope ratio signatures in argillaceous and dolomitic limestones (especially for samples satisfying all three criteria: Mg/Ca < 0.4 g g^{-1}, Mn/Sr < 2 g g^{-1} and Sr/(Ca+Mg) > 200 μg g^{-1}) where the other established procedures failed. However, no significant differences were evident

for high purity, and low Mg/Ca limestones, which underlines the importance of matching different sample types to the most appropriate dissolution method.

(5) Thresholds for using Mg/Ca, [Sr] and Mn/Sr as screening tools for SIS study are recommended: Mg/Ca < 0.4 (preferably < 0.25) g g^{-1}; [Sr] > 200 (preferably > 400) µg g^{-1}; Mn/Sr < 2 g g^{-1}. Our leaching method increases the likelihood significantly of obtaining close to seawater Sr isotopic value for samples with carbonate content < 70% when other thresholds are met.

Acknowledgements

Data availability statement

The data that support the findings of this study are available in the supplementary material of this article

References

Bailey T.R., McArthur J.M., Prince H. and Thirlwall M.F. (2000)

Dissolution methods for strontium isotope stratigraphy: Whole rock analysis. **Chemical Geology, 167,** 313–319.

Banner J.L. and Hanson G.N. (1990)

Calculation of simultaneous isotopic and trace element variations during water-rock interaction with applications to carbonate diagenesis. **Geochimica et Cosmochimica Acta, 54**, 3123–3137.

Banner J.L., Hanson G.N. and Meyers W.J. (1988)

Rare earth element and Nd isotopic variations in regionally extensive dolomites from the Burlington-Keokuk Formation (Mississippian): Implications for REE mobility during carbonate diagenesis. **Journal of Sedimentary Petrology, 58,** 415–432.

Bartley J.K., Semikhatov M.A., Kaufman A.J., Knoll A.H., Pope M.C. and Jacobsen S.B. (2001)

Global events across the Mesoproterozoic-Neoproterozoic boundary: C and Sr isotopic evidence from Siberia. **Precambrian Research, 111,** 165–202.

Bellefroid E.J., Planavsky N.J., Miller N.R., Brand U. and Wang C. (2018)
Case studies on the utility of sequential carbonate leaching for radiogenic strontium isotope analysis. **Chemical Geology, 497**, 88–99.

Bold U., Smith E.F., Rooney A.D., Bowring S.A., Buchwaldt R., Dudás F.O., Ramezani J., Crowley J.L., Schrag D.P. and Macdonald F.A. (2016)
Neoproterozoic stratigraphy of the Zavkhan terrane of Mongolia: The backbone for Cryogenian and early Ediacaran chemostratigraphic records. **American Journal of Science, 315,** 1–63.

Brand U., Azmy K., Tazawa J.I., Sano H. and Buhl D. (2010)
Hydrothermal diagenesis of Paleozoic seamount carbonate components. **Chemical Geology, 278**, 173–185.

Broecker W.S. and Peng T.H. (1983)
Tracers in the sea. **Eldigio Press (New York),** 690pp.

Burke W.H., Denison R.E., Hetherington E.A., Koepnick R.B., Nelson H.F. and Otto J.B. (1982)
Variation of seawater $^{87}Sr/^{86}Sr$ throughout Phanerozoic time. **Geology, 10**, 516–519.

Cao C., Liu X.M., Bataille C.P. and Liu C. (2020)
What do Ce anomalies in marine carbonates really mean? A perspective from leaching experiments. **Chemical Geology, 532,** 119413.

Cawood P.A., Hawkesworth C.J., Pisarevsky S.A., Dhuime B., Capitanio F.A. and Nebel O. (2018)

Geological archive of the onset of plate tectonics. **Philosophical Transactions of the Royal Society A, 376,** 20170405.

Chen J., Algeo T.J., Zhao L., Chen Z.Q., Cao L., Zhang L. and Li Y. (2015)

Diagenetic uptake of rare earth elements by bioapatite, with an example from Lower Triassic conodonts of south China. **Earth-Science Reviews**, **149,** 181–202.

Chen X., Zhou Y. and Shields G.A. (2022)

Progress towards an improved Precambrian seawater $^{87}Sr/^{86}Sr$ curve. **Earth-Science Reviews, 224**, 103869.

Chilingar G.V. (1957)

Classification of limestones and dolomites on basis of Ca/Mg ratio. **Journal of Sedimentary Petrology, 27,** 187–189.

Cox G.M., Halverson G.P., Stevenson R.K., Vokaty M., Poirier A., Kunzmann M., Li Z. X., Denyszyn S.W., Strauss J. v. and Macdonald F.A. (2016)

Continental flood basalt weathering as a trigger for Neoproterozoic Snowball Earth. **Earth and Planetary Science Letters, 446,** 89–99.

Cui H., Kaufman A.J., Xiao S., Zhu M., Zhou C. and Liu X.M. (2015)

Redox architecture of an Ediacaran ocean margin: Integrated chemostratigraphic (δ^{13}C-δ^{34}S-^{87}Sr/^{86}Sr-Ce/Ce*) correlation of the Doushantuo Formation, south China. **Chemical Geology, 405,** 48–62.

Cui H., Kaufman A.J., Zou H., Kattan F.H., Trusler P., Smith J., Yu. Ivantsov A., Rich T.H., al Qubsani A., Yazedi A., Liu X.M., Johnson P., Goderis S., Claeys P. and Vickers-Rich P. (2020)

Primary or secondary? A dichotomy of the strontium isotope anomalies in the Ediacaran carbonates of Saudi Arabia. **Precambrian Research, 343**, 105720.

Elderfield H. (1986)

Strontium isotope stratigraphy. **Palaeogeography, Palaeoclimatology, Palaeoecology, 57**, 71–90.

Fairchild I.J., Spencer A.M., Ali D.O., Anderson R.P., Anderton R., Boomer I., Dove D., Evans J.D., Hambrey M.J., Howe J., Sawaki Y., Shields G.A., Skelton A., Tucker M.E., Wang Z. and Zhou Y. (2018)

Tonian-Cryogenian boundary sections of Argyll, Scotland. **Precambrian Research, 319**, 37–64.

Gibson T.M., Wörndle S., Crockford P.W., Bui T.H., Creaser R.A. and Halverson G.P. (2019)

Radiogenic isotope chemostratigraphy reveals marine and nonmarine depositional environments in the late Mesoproterozoic Borden Basin, Arctic Canada. **Geological Society of America Bulletin, 11,** 1965–1978.

Gonneea M.E. and Paytan A. (2006)

Phase associations of barium in marine sediments. **Marine Chemistry, 100,** 124-135.

Gorokhov I., Semikhatov M., Baskakov A., Kutyavin E., Mel'Nikov N., Sochava A. and Turchenko T. (1995)

Sr isotopic composition in Riphean, Vendian and Lower Cambrian carbonates from Siberia. **Stratigraphy and Geological Correlation, 3,** 1–28.

Guo H., Du Y., Kah L.C., Huang J., Hu C., Huang H. and Yu W. (2013)

Isotopic composition of organic and inorganic carbon from the Mesoproterozoic Jixian Group, north China: Implications for biological and oceanic evolution. **Precambrian Research, 224**, 169–183.

Halverson G.P. (2007)

A Neoproterozoic chronology. **Neoproterozoic Geobiology and Paleobiology, 27,** 231–271.

Halverson G.P., Dudás F.Ö., Maloof A.C. and Bowring S.A. (2007)

Evolution of the ^{87}Sr/^{86}Sr composition of Neoproterozoic seawater.

Palaeogeography, Palaeoclimatology, Palaeoecology, 256, 103–129.

Hawkesworth C.J., Cawood P.A. and Dhuime B. (2016)

Tectonics and crustal evolution. **GSA Today, 26,** 4–11.

Hodell D.A., Mead G.A. and Mueller P.A. (1990)

Variation in the strontium isotopic composition of seawater (8 Ma to present):

Implications for chemical weathering rates and dissolved fluxes to the oceans.

Chemical Geology: Isotope Geoscience Section, 80, 291–307.

James R.H., Elderfield H. and Palmer M.R. (1995)

The chemistry of hydrothermal fluids from the Broken Spur site, 29°N Mid-

Atlantic ridge. **Geochimica et Cosmochimica Acta, 59,** 651–659.

Kah L.C., Lyons T.W. and Chesley J.T. (2001)

Geochemistry of a 1.2 Ga carbonate-evaporite succession, northern Baffin and

Bylot Islands: Implications for Mesoproterozoic marine evolution. **Precambrian**

Research, 111, 203–234.

Kamber B.S., Greig A. and Collerson K.D. (2005)

A new estimate for the composition of weathered young upper continental crust

from alluvial sediments, Queensland, Australia. **Geochimica et Cosmochimica**

Acta, 69, 1041–1058.

Kaufman A.J. and Knoll A.H. (1995)

Neoproterozoic variations in the C-isotopic composition of seawater: Stratigraphic and biogeochemical implications. **Precambrian Research, 73**, 27–49.

Kuznetsov A.B., Melezhik V.A., Gorokhov I.M., Melnikov N.N., Konstantinova G. v., Kutyavin E.P. and Turchenko T.L. (2010)
Sr isotopic composition of Paleoproterozoic ^{13}C-rich carbonate rocks: The Tulomozero Formation, SE Fennoscandian Shield. **Precambrian Research, 182,** 300–312.

Kuznetsov A.B., Ovchinnikova G. v., Semikhatov M.A., Gorokhov I.M., Kaurova O.K., Krupenin M.T., Vasil'eva I.M., Gorokhovskii B.M. and Maslov A. v. (2008)
The Sr isotopic characterization and Pb-Pb age of carbonate rocks from the Satka formation, the Lower Riphean Burzyan Group of the southern Urals. **Stratigraphy and Geological Correlation, 16,** 120–137.

Kuznetsov A.B., Semikhatov M.A. and Gorokhov I.M. (2012)
The Sr isotope composition of the world ocean, marginal and inland seas: Implications for the Sr isotope stratigraphy. **Stratigraphy and Geological Correlation, 20,** 501–515.

Li D., Shields-Zhou G.A., Ling H.F. and Thirlwall M. (2011)
Dissolution methods for strontium isotope stratigraphy: Guidelines for the use of bulk carbonate and phosphorite rocks. **Chemical Geology, 290**, 133–144.

Li Y., Li C. and Guo J. (2020)

Re-evaluation and optimisation of dissolution methods for strontium isotope stratigraphy based on chemical leaching of carbonate certificated reference materials. **Microchemical Journal, 154,** 104607.

Liu C., Wang Z. and Raub T.D. (2013)

Geochemical constraints on the origin of Marinoan cap dolostones from Nuccaleena Formation, South Australia. **Chemical Geology, 351,** 95–104.

Liu C., Wang Z., Raub T.D., Macdonald F.A. and Evans D.A.D. (2014)

Neoproterozoic cap-dolostone deposition in stratified glacial meltwater plume. **Earth and Planetary Science Letters, 404,** 22–32.

Mazzullo S.J. (1992)

Geochemical and neomorphic alteration of dolomite: A review. **Carbonates and Evaporites, 7,** 21–37.

McArthur J.M. (1994)

Recent trends in strontium isotope stratigraphy. **Terra Nova, 6,** 331–358.

McArthur J.M., Howarth R.J. and Shields G.A. (2012)

Strontium isotope stratigraphy. **In: Gradstein F.M., Ogg J.G., Schmitz M.B. and Ogg, G.M. (eds), The geologic time scale 2012. Elsevier,** 127–144.

McCulloch M.T. (1994)

Primitive $^{87}Sr^{86}Sr$ from an Archean barite and conjecture on the Earth's age and origin. **Earth and Planetary Science Letters, 126,** 1–13.

Mei M. (2005)

Preliminary study on sequence-stratigraphic position and origin for molar-tooth structure of the Gaoyuzhuang Formation of Mesoproterozoic at Jixian section in Tianjin. **Journal of Palaeogeography, 7,** 437–447.

Melezhik V.A., Gorokhov I.M., Fallick A.E. and Gjelle S. (2001)

Strontium and carbon isotope geochemistry applied to dating of carbonate sedimentation: An example from high-grade rocks of the Norwegian Caledonides. **Precambrian Research, 108,** 267–292.

Meyer A.C.S., Grundle D. and Cullen J.T. (2021)

Selective uptake of rare earth elements in marine systems as an indicator of and control on aerobic bacterial methanotrophy. **Earth and Planetary Science Letters, 558,** 116756.

Miller N., Johnson P.R. and Stern R.J. (2008)

Marine versus non-marine environments for the Jibalah Group, NW Arabian shield: A sedimentologic and geochemical survey and report of possible metazoa in the Dhaiqa Formation. **Arabian Journal for Science and Engineering, 33,** 55-77.

Moldoveanu G.A. and Papangelakis V.G. (2013)

Recovery of rare earth elements adsorbed on clay minerals: II. Leaching with ammonium sulfate. **Hydrometallurgy, 131–132**, 158-166.

Montañez I.P., Banner J.L., Osleger D.A., Borg L.E. and Bosserman P.J. (1996)

Integrated Sr isotope variations and sea-level history of middle to Upper Cambrian platform carbonates: Implications for the evolution of Cambrian seawater $^{87}Sr/^{86}Sr$. **Geology, 24**, 917.

Nothdurft L.D., Webb G.E. and Kamber B.S. (2004)

Rare earth element geochemistry of Late Devonian reefal carbonates, Canning Basin, Western Australia: Confirmation of a seawater REE proxy in ancient limestones. **Geochimica et Cosmochimica Acta, 68,** 263–283.

Nozaki Y., Zhang J. and Amakawa H. (1997)

The fractionation between Y and Ho in the marine environment. **Earth and Planetary Science Letters, 148,** 329–340.

Pogge von Strandmann P.A.E., Jenkyns H.C. and Woodfine R.G. (2013)

Lithium isotope evidence for enhanced weathering during Oceanic Anoxic Event 2. **Nature Geoscience, 6,** 668–672.

Pourmand A., Dauphas N. and Ireland T.J. (2012)

A novel extraction chromatography and MC-ICP-MS technique for rapid analysis of REE, Sc and Y: Revising CI-chondrite and Post-Archean Australian Shale (PAAS) abundances. **Chemical Geology, 291,** 38–54.

Ray J.S., Veizer J. and Davis W.J. (2003)

C, O, Sr and Pb isotope systematics of carbonate sequences of the Vindhyan Supergroup, India: Age, diagenesis, correlations and implications for global events. **Precambrian Research, 121**, 103–140.

Renwei L., Jenshi C., Shukun Z. and Zhimig C. (2003)

Secular variations in carbon isotopic compositions of carbonates from Proterozoic successions in the Ming Tombs section of the North China Platform. **Journal of Asian Earth Sciences, 22,** 329–341.

Roerdink D.L., Ronen Y., Strauss H. and Mason P.R.D. (2022)

Emergence of felsic crust and subaerial weathering recorded in Palaeoarchaean barite. **Nature Geoscience, 15,** 227–232.

Rutten A. and de Lange G.J. (2002)

A novel selective extraction of barite, and its application to eastern Mediterranean sediments. **Earth and Planetary Science Letters, 198,** 1–2.

Satkoski A.M., Fralick P., Beard B.L. and Johnson C.M. (2017)

Initiation of modern-style plate tectonics recorded in Mesoarchean marine chemical sediments. **Geochimica et Cosmochimica Acta, 209,** 216–232.

Satkoski A.M., Lowe D.R., Beard B.L., Coleman M.L. and Johnson C.M. (2016)

A high continental weathering flux into Paleoarchean seawater revealed by strontium isotope analysis of 3.26 Ga barite. **Earth and Planetary Science Letters, 454,** 28–35.

Shields G.A. (2007)

A normalised seawater strontium isotope curve: Possible implications for Neoproterozoic-Cambrian weathering rates and the further oxygenation of the Earth. **eEarth, 2,** 35–42.

Shields G. and Veizer J. (2002)

Precambrian marine carbonate isotope database: Version 1.1. **Geochemistry, Geophysics, Geosystems, 3**.

Spooner E.T.C. (1976)

The strontium isotopic composition of seawater, and seawater-oceanic crust interaction. **Earth and Planetary Science Letters, 31,** 167–174.

Stammeier J.A., Nebel O., Hippler D. and Dietzel M. (2020)

A coherent method for combined stable magnesium and radiogenic strontium isotope analyses in carbonates (with application to geological reference materials SARM 40, SARM 43, SRM 88A, SRM 1B). **MethodsX, 7,** 100847.

Stüeken E.E., Bellefroid E.J., Prave A., Asael D., Planavsky N.J. and Lyons T.W. (2017)

Not so non-marine? Revisiting the Stoer Group and the Mesoproterozoic biosphere. **Geochemical Perspectives Letters, 3,** 221–229.

Tan C., Lu Y., Li X., Song H., Lv D., Ma X., Fan R. and Deng S. (2020)

Carbon, oxygen and strontium isotopes of the Mesoproterozoic Jixian System (1.6–1.4 Ga) in the southern margin of the North China Craton and the geological implications. **International Geology Review, 00,** 1–18.

Taylor S.R. and McLennan S.M. (1981)

The rare earth element evidence in Precambrian sedimentary rocks: Implications for crustal evolution. **Developments in Precambrian Geology, 4.**

Tessier A., Campbell P.G.C. and Bisson M. (1979)

Sequential extraction procedure for the speciation of particulate trace metals. **Analytical Chemistry, 51,** 844–851.

Tostevin R., Shields G.A., Tarbuck G.M., He T., Clarkson M.O. and Wood R.A. (2016)

Effective use of cerium anomalies as a redox proxy in carbonate-dominated marine settings. **Chemical Geology, 438,** 146–162.

Vahrenkamp V.C. and Swart P.K. (1990)

New distribution coefficient for the incorporation of strontium into dolomite and its implications for the formation of ancient dolomites. **Geology, 18**, 387–391.

Veizer J. (1989)

Strontium isotopes in seawater through time. **Annual Review of Earth and Planetary Sciences, 17,** 141–167.

Veizer J., Ala D., Azmy K., Bruckschen P., Buhl D., Bruhn F., Garden G.A.F., Diener A., Ebneth S., Godderis Y., Jasper T., Korte C., Pawellek F., Podlaha O.G. and Strauss H. (1999)

$^{87}Sr/^{86}Sr$, $\delta^{13}C$ and $\delta^{18}O$ evolution of Phanerozoic seawater. **Chemical Geology**, **161**, 59–88.

Verdel C., Phelps B. and Welsh K. (2018)

Rare earth element and $^{87}Sr/^{86}Sr$ step-leaching geochemistry of central Australian Neoproterozoic carbonate. **Precambrian Research, 310,** 229–242.

Webb G.E. and Kamber B.S. (2000)

Rare earth elements in Holocene reefal microbialites: A new shallow seawater proxy. **Geochimica et Cosmochimica Acta, 64**, 1557–1565.

Weis D., Kieffer B., Maerschalk C., Barling J., De Jong J., Williams G.A., Hanano D., Pretorius W., Mattielli N., Scoates J.S. and Goolaerts A. (2006)

High-precision isotopic characterization of USGS reference materials by TIMS and MC-ICP-MS. **Geochemistry, Geophysics, Geosystems, 7**.

Wierzbowski H., Anczkiewicz R., Bazarnik J. and Pawlak J. (2012)

Strontium isotope variations in Middle Jurassic (Late Bajocian-Callovian) seawater: Implications for Earth's tectonic activity and marine environments. **Chemical Geology, 334**, 171–181.

Zhang K. and Shields G.A. (2022)

Sedimentary Ce anomalies: Secular change and implications for paleoenvironmental evolution. **Earth-Science Reviews, 229,** 104015.

Zhang K., Zhu X.K. and Yan B. (2015)

A refined dissolution method for rare earth element studies of bulk carbonate rocks. **Chemical Geology, 412,** 82–91.

Zhang K., Zhu X., Wood R.A., Shi Y., Gao, Z. and Poulton S.W. (2018)

Oxygenation of the Mesoproterozoic ocean and the evolution of complex eukaryotes. **Nature Geoscience, 11,** 345–350.

Zhong S. and Mucci A. (1995)

Partitioning of rare earth elements (REEs) between calcite and seawater solutions at 25 °C and 1 atm, and high dissolved REE concentrations**. Geochimica et Cosmochimica Acta, 59,** 443–453.

Zhou Y., Pogge von Strandmann P.A.E., Zhu M., Ling H., Manning C., Li D., He T. and Shields G.A. (2020)

Reconstructing Tonian seawater $^{87}Sr/^{86}Sr$ using calcite microspar. **Geology, 48, 462–467.**

Supporting information

The following supporting information may be found in the online version of this article:

Table S1. Step-leaching elemental ratios of argillaceous and dolomitic limestones and two rock reference materials.

Table S2. Step-leaching REY data of argillaceous and dolomitic limestones.

Figure S1. Cross plots of Ba/Sm and Eu_{sn}/Eu^*_{sn} for five argillaceous and dolomitic limestones.

Figure S2. Cross-plot of stepwise Rb/Sr *versus* Ba/Ca ratios for each argillaceous and dolomitic limestone.

This material is available from:

http://onlinelibrary.wiley.com/doi/10.1111/ggr.00000/abstract

(This link will take you to the article abstract).

Figure captions

Figure 1. Stepwise leaching pattern. (a) Leaching patterns for the argillaceous and slightly dolomitic limestone (SDL) J95, G99, K46; (b) Leaching patterns for the argillaceous and highly dolomitic limestone (HDL) G90, HXSZ4; (c) Leaching pattern for the pure limestone rock reference material LS19; (d) Leaching pattern for pure dolostone CRM 88a.

Figure 2. Ten-step REY leaching pattern for argillaceous and dolomitic limestones. S1–S9: Each plot shows each step, and lines with different colours represent different samples. The modern seawater REY pattern is from Zhang and Shields (2022). All plots are in log scale. Except for G99, all samples show the seawater like pattern in S1 (some also in S2).

Figure 3. Y/Ho ratios in each leaching step of each sample. All samples in S1 show Y/Ho > 36 (seawater signal; less clay contamination).

Figure 4. (a) Strontium isotope results by applying three different leaching Methods to each sample. Method 1 (this study) – target the first 10–30% after NH$_4$Ac prewash; Method 2 – pre-leach 30%, target the next 30%, developed mainly for high purity limestone (Bailey *et al.* 2000, Li *et al.* 2011); Method 3 – pre-leach 60–70%, target the next ~ 20%, developed for dolostone (Liu *et al.* 2013, Li *et al.* 2020). Blue horizontal bar presents the proposed seawater range from ~ 0.7046 to ~ 0.7056 of the Member III of the Gaoyuzhuang Formation

(e.g., Ray *et al.* 2003, Kuznetsov *et al.* 2008, Bellefroid *et al.* 2018, Tan *et al.* 2020). (b) Bulk Mg/Ca ratios of samples range from 0.01 to 0.6. (c) Carbonate content of each sample. Redline shows % carbonate = 80%, which divides samples into high purity (> 80%) and low purity (< 80%).

Figure 5. Cross-plots of stepwise Rb/Sr, Mn/Sr and Mg/Ca ratios versus Sr isotopes for each argillaceous and dolomitic limestone. After S0 (prewash), correlations of Rb/Sr, Mn/Sr and Mg/Ca ratios with $^{87}Sr/^{86}Sr$ isotope ratios from S1 to S9 are shown in blue lines.

Figure 6. Recommended protocol from this study, for effective leaching of primary $^{87}Sr/^{86}Sr$ isotope ratios from argillaceous and dolomitic limestone.

Figure 7. Cross-plots bulk rock parameters of samples versus their lowermost Sr isotopes among three leaching cut-offs (see Table 4 for data). The blue shades show a seawater $^{87}Sr/^{86}Sr$ range (0.7046–0.7056) during this period. The yellow shades and red solid lines represent the thresholds highly probable for samples to yield seawater values. The red dash line shows recommended thresholds.

Table 1. Bulk carbonate information for samples used for step-leaching experiments

Sample Labels	Sample types	Carbonate content (%)	Mg/Ca (g g^{-1})	Mn/Sr (g g^{-1})	Rb/Sr (mg g^{-1})	K/Ca (mg g^{-1})	Al/Ca (mg g^{-1})	Ba/Ca (mg g^{-1})	Fe/Ca (mg g^{-1})	[Sr/Ca+Mg] (μg g^{-1})	$\delta^{13}C_{VPDB}$ (‰)	$\delta^{18}O_{VPDB}$ (‰)	Age (Ga)
LS19	LST	90	0.02	0.03	10	0.38	0.39	0.01	0.10	988			~ 0.96
J95	SDL	70	0.06	0.14	5.48	0.79	2.15	0.06	2.02	672	-0.64	-5.25	~ 1.56–1.57
G99	SDL	57	0.11	0.51	36.90	4.75	5.73	0.19	17.84	876	-1.41	-5.82	~ 1.56–1.57
K46	SDL	75	0.20	0.34	11.47	1.73	3.43	0.09	5.91	661	-0.57	-5.54	~ 1.56–1.57
G90	HDL	62	0.40	1.31	30.67	2.01	2.80	0.09	14.12	368	-0.99	-3.49	~ 1.56–1.57
HXSZ4	HDL	62	0.30	0.28	6.88	1.28	2.46	0.11	6.89	519	-0.52	-4.21	~ 1.56–1.57
88a	DST	98	0.6	4.83	3.02	4.60	4.00	0.01	9.00	121			

Table 2. Sequential leaching protocol. Six-step leaching (design to dissolve 20% carbonate in each step after pre-wash) was conducted for pure limestone (LST); and ten-step leaching (designed to dissolve 10% carbonate in each step after pre-wash) was conducted for SDL, HDL, DST. pH of each reagent: 1 mol l^{-1} NH$_4$HAc (~ 7); 0.05 mol l^{-1} HAc (~ 3); 0.2 mol l^{-1} HAc (~ 2.7); 0.5 mol l^{-1} HAc (~ 2.5). usb: ultrasonic bath. HAc: acetic acid.

Steps	LST	SDL	HDL	DST	Reaction time
S0	5 ml of 1 mol l^{-1} NH$_4$HAc	5 ml of 1 mol l^{-1} NH$_4$HAc	5 ml of 1 mol l^{-1} NH$_4$HAc	5 ml of 1 mol l^{-1} NH$_4$HAc	30 min usb at room temperature
S1-S2	7.5 ml of 0.05 mol l^{-1} HAc	4 ml of 0.2 mol l^{-1} HAc	2.5 ml of 0.5 mol l^{-1} HAc	5 ml of 0.5 mol l^{-1} HAc	30 min usb + 30 min stand at room temperature
S3-S5	7.5 ml of 0.05 mol l^{-1} HAc	5 ml of 0.2 mol l^{-1} HAc	3.5 ml of 0.5 mol l^{-1} HAc	8 ml of 0.5 mol l^{-1} HAc	30 min -1 h usb + 30 min -1 h stand at room temperature
S6-S8		8 ml of 0.2 mol l^{-1} HAc	6 ml of 0.5 mol l^{-1} HAc	10 ml of 0.5 mol l^{-1} HAc	2 h usb + 2 hr stand at 30–40 °C
S9		10 ml of 0.5 mol l^{-1} HAc	10 ml of 0.5 mol l^{-1} HAc	10 ml of 0.5 mol l^{-1} HAc	Overnight on mixing roller at room temperature

Table 3.							
$^{87}Sr/^{86}Sr$ isotope ratios and cumulative carbonate dissolution in each step of each sample							
Sample	**Carbonate disso**	**$^{87}Sr/^{86}Sr$**	**2SE**	**Sample**	**Carbonate disso (cumulative)**	**$^{87}Sr/^{86}Sr$**	**2SE**
LS19-0	5.64%	0.70595	0.000025	G90-0	5.02%	0.71029	0.000023
LS19-1	28.34%	*0.70543*	0.00002	G90-1	25.93%	*0.70533*	0.000022
LS19-2	50.84%	*0.70543*	0.000021	G90-2	33.77%	0.7058	0.000022
LS19-3	72.89%	*0.70543*	0.000023	G90-3	41.96%	0.70704	0.000025
LS19-4	87.93%	0.70545	0.000022	G90-4	50.69%	0.70781	0.000025
LS19-5	98.00%	0.70565	0.000025	G90-5	58.38%	0.7078	0.000025
J95-0	5.16%	0.70669	0.000027	G90-6	65.64%	0.7081	0.000019
J95-1	17.34%	*0.70503*	0.000021	G90-7	75.14%	0.7077	0.000023
J95-2	32.20%	0.70509	0.000023	G90-8	86.00%	0.7076	0.000018
J95-3	40.10%	0.70511	0.00002	G90-9	95.00%	0.71025	0.000024
J95-4	49.29%	0.7051	0.000018	HXSZ4-0	8.35%	0.70808	0.000024
J95-5	63.12%	0.70529	0.000021	HXSZ4-1	22.00%	*0.7052*	0.000026
J95-6	70.49%	0.70534	0.000017	HXSZ4-2	34.00%	*0.70522*	0.000024
J95-7	77.78%	0.70544	0.000021	HXSZ4-3	46.00%	0.70561	0.00002
J95-8	86.00%	0.7063	0.000021	HXSZ4-4	55.00%	0.70629	0.000021
J95-9	96.00%	0.7069	0.000019	HXSZ4-5	65.00%	0.70631	0.000018
G99-0	6.09%	0.71089	0.000023	HXSZ4-6	74.00%	0.70667	0.000019
G99-1	28.00%	*0.70508*	0.000025	HXSZ4-7	80.00%	0.70704	0.000018
G99-2	41.88%	0.70525	0.00003	HXSZ4-8	87.00%	0.7068	0.000025
G99-3	50.00%	0.70628	0.000027	HXSZ4-9	96.00%	0.71075	0.000028
G99-4	56.00%	0.70741	0.000025	88a-0	1.10%	0.71051	0.000025
G99-5	65.00%	0.70737	0.00002	88a-1	13.87%	0.71016	0.000014
G99-6	74.00%	0.70889	0.00002	88a-2	29.05%	0.71016	0.000021
G99-7	85.00%	0.70936	0.000022	88a-3	39.64%	0.71039	0.000026
G99-8	90.00%	0.71017	0.000023	88a-4	48.63%	0.7104	0.000025
G99-9	98.00%	0.71017	0.000029	88a-5	61.29%	0.71044	0.000026
K46-0	6.51%	0.71301	0.00002	88a-6	73.36%	0.71048	0.000018
K46-1	28.00%	*0.70507*	0.00003	88a-7	83.97%	*0.71004*	0.000024
K46-2	38.00%	0.70522	0.00002	88a-8	90.63%	*0.71005*	0.000028
K46-3	50.00%	0.70803	0.000024	88a-9	93.81%	0.71009	0.000023
K46-4	61.00%	0.708	0.000029				
K46-5	70.00%	0.7079	0.000024				
K46-6	79.00%	0.7078	0.000027				
K46-7	87.00%	0.7077	0.000021				
K46-8	94.00%	0.7081	0.000021				
K46-9	97.00%	0.7099	0.000021				

The "internal" standard error (2SE) for each sample is reported in the table. LS19, J95, G99, K46 were measured in one session within which the repeatability for NBS 987 is 0.000031 (2s, N = 72); G90, HXSZ4, 88a were measured in one session within which the repeatability for NBS 987 is 0.000030 (2s, N

= 60). The lowest value (within 2SE) for each sample is highlighted by bold and italic. See Table S1 for major and trace element data.

Table 4.

$^{87}Sr/^{86}Sr$ isotope ratios of applying different cut-offs to samples with various bulk rock information

| Samples	$^{87}Sr/^{86}Sr$			Bulk rock			
	Method 1	Method 2	Method 3	Carbonate content	Mg/Ca (g g^{-1})	Mn/Sr (g g^{-1})	[Sr/(Ca+Mg)] (µg g^{-1})
HXS1	*0.70487* (± 0.00	*0.70488* (± 0.00	*0.70488* (± 0.00	91.49	0.01	0	8295.27
J56	*0.70569* (± 0.00	*0.70570* (± 0.00	*0.70601* (± 0.00	56.06	0.02	0.31	579.2
K68	*0.70493* (± 0.00	*0.70495* (± 0.00	0.70508 (± 0.000	84.95	0.07	0.35	521.65
G176	*0.70653* (± 0.00	0.70809 (± 0.000	*0.70655* (± 0.00	87.55	0.07	3.04	192.74
G94	*0.70498* (± 0.00	0.70577 (± 0.000	0.71191 (± 0.000	49.2	0.13	0.23	1106.69
K66	*0.70496* (± 0.00	0.70536 (± 0.000	0.70596 (± 0.000	87.62	0.19	0.3	662.06
G97	*0.70509* (± 0.00	0.70689 (± 0.000	0.71325 (± 0.000	49.52	0.26	0.48	662.05
G114	0.70829 (± 0.000	*0.70800* (± 0.00	0.70891 (± 0.000	48.06	0.28	2.22	404.09
K69	*0.70583* (± 0.00	0.70692 (± 0.000	0.70771 (± 0.000	70	0.28	0.4	779.79
G151	*0.71038* (± 0.00	0.71086 (± 0.000	*0.70723* (± 0.00	57.45	0.3	3.82	233.93
K73.5	*0.70503* (± 0.00	*0.70505* (± 0.00	0.70643 (± 0.000	88	0.31	0.44	842.47
K82	*0.70520* (± 0.00	0.70592 (± 0.000	0.70616 (± 0.000	66.94	0.33	0.56	442.54
P60	*0.70483* (± 0.00	0.70674 (± 0.000	*0.70484* (± 0.00	84.2	0.34	1.69	218.06
K49	*0.70559* (± 0.00	0.70595 (± 0.000	0.70647 (± 0.000	81.8	0.37	0.84	389.22
K65	*0.70535* (± 0.00	0.70546 (± 0.000	0.70687 (± 0.000	84.59	0.39	0.67	499.8
J46	*0.70662* (± 0.00	0.70700 (± 0.000	0.70724 (± 0.000	70.28	0.4	4.43	261.99
SSAZ19	0.71053 (± 0.000	*0.70798* (± 0.00	0.70812 (± 0.000	72.86	0.44	2	301.35
P68	*0.70802* (± 0.00	0.70857 (± 0.000	0.70959 (± 0.000	62.13	0.46	3.34	178.26
P64	0.70731 (± 0.000	0.70816 (± 0.000	*0.70600* (± 0.00	92.21	0.49	2.89	145.95
G60	0.70806 (± 0.000	0.71173 (± 0.000	*0.70723* (± 0.00	59.46	0.6	4.29	124.37

Note that the number in the bracket represents 2SE. **Bold and italic** highlight the lowest value (within 2SE) among three different leaching methods. Repeatability (for NBS 987) is 0.000031 (2s, N = 4
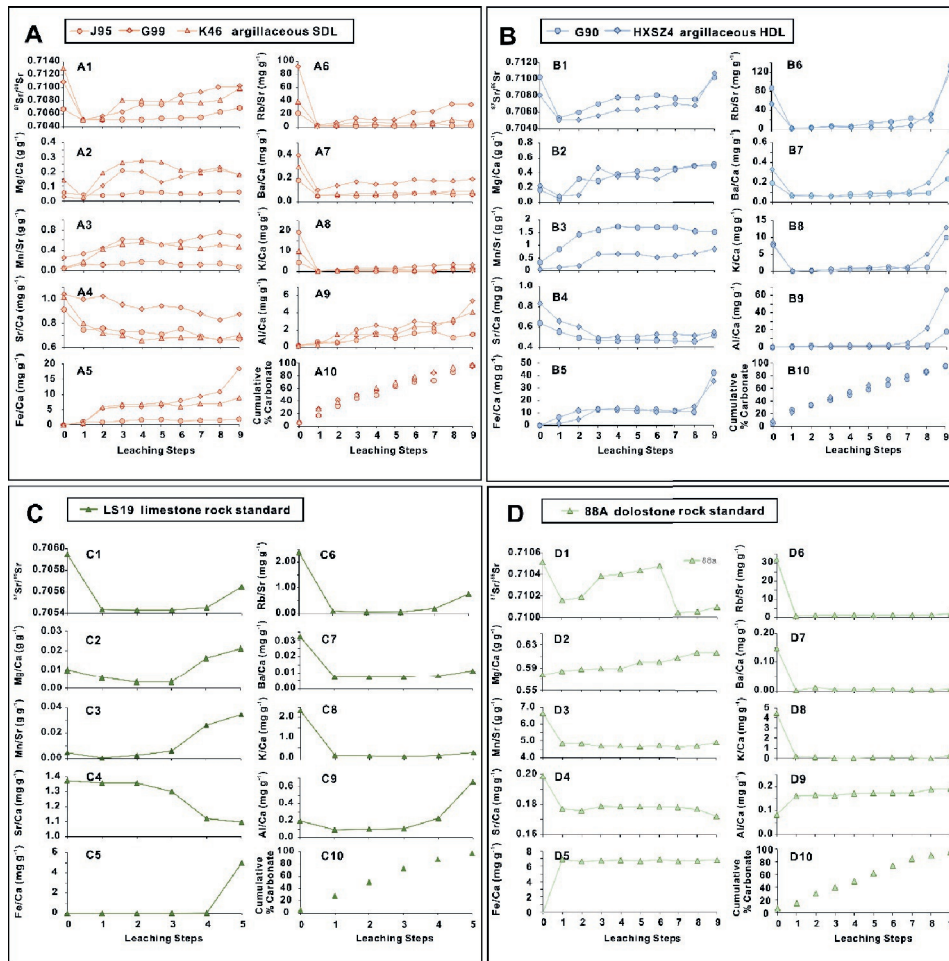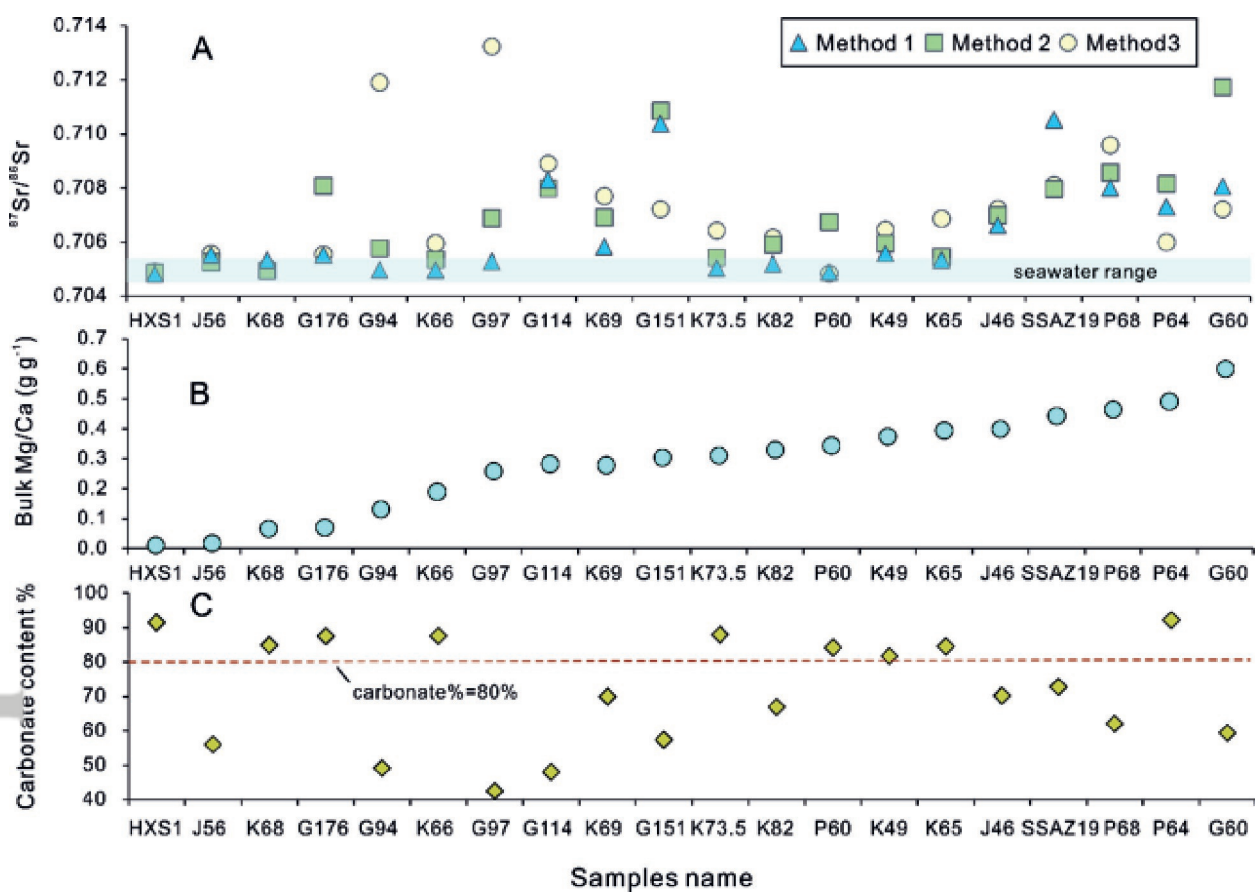
ggr_1000_fig1_temp.eps
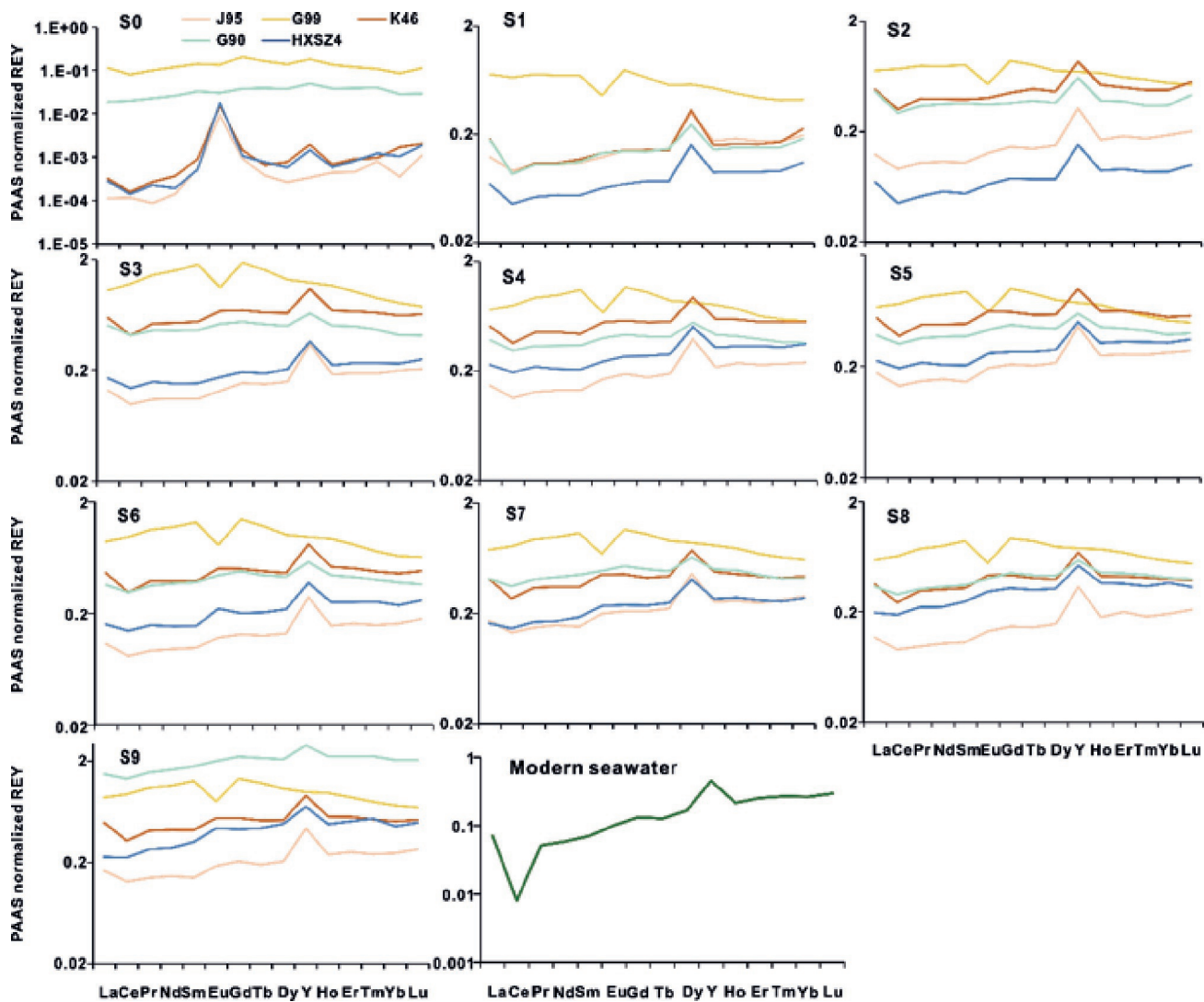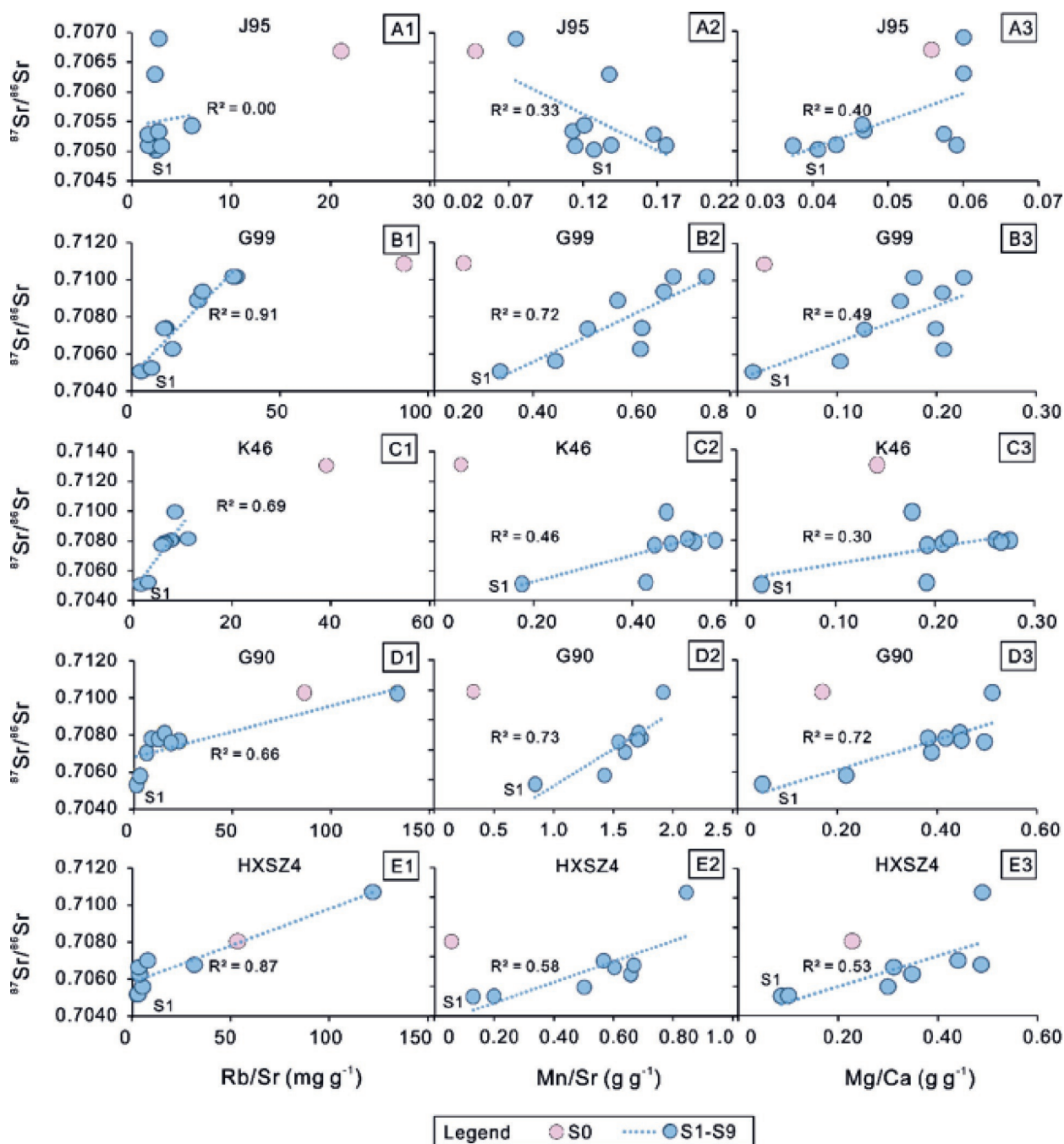
ggr_1000_fig2_temp.eps
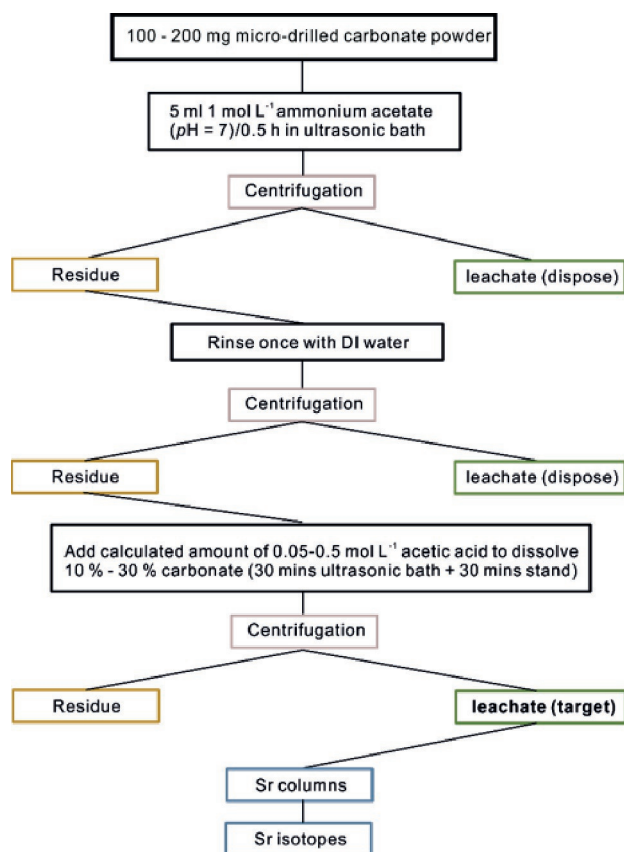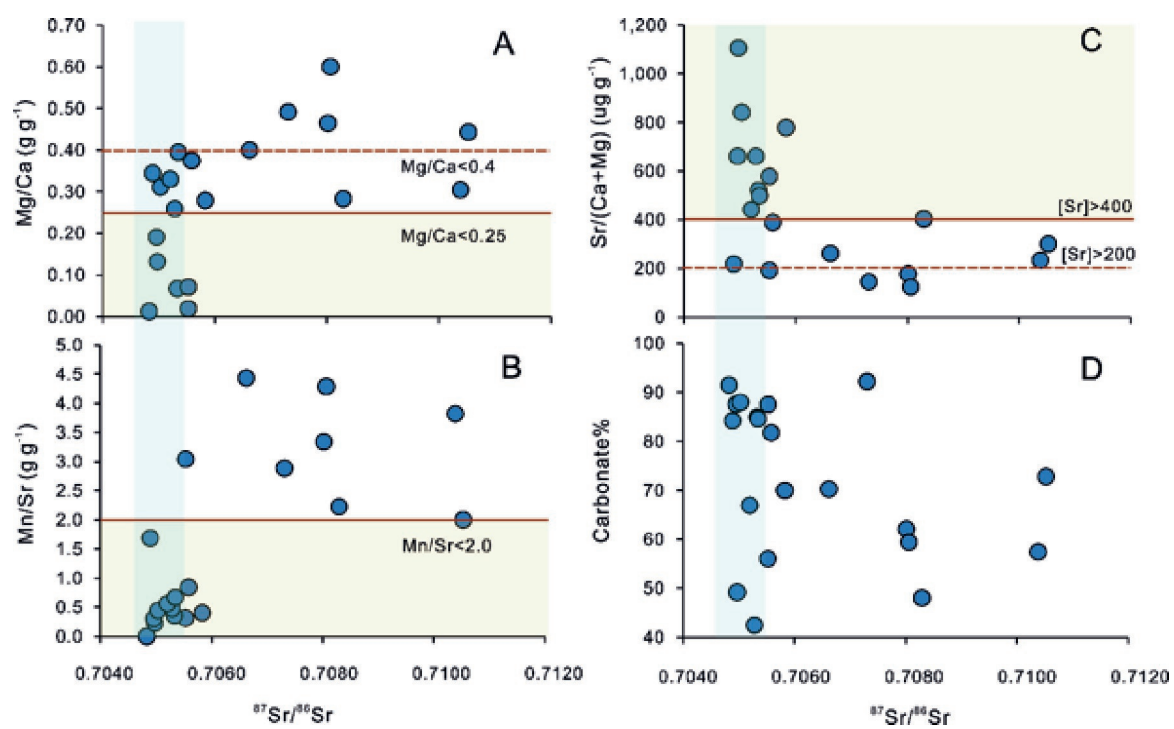
ggr_1000_fig3_temp.eps
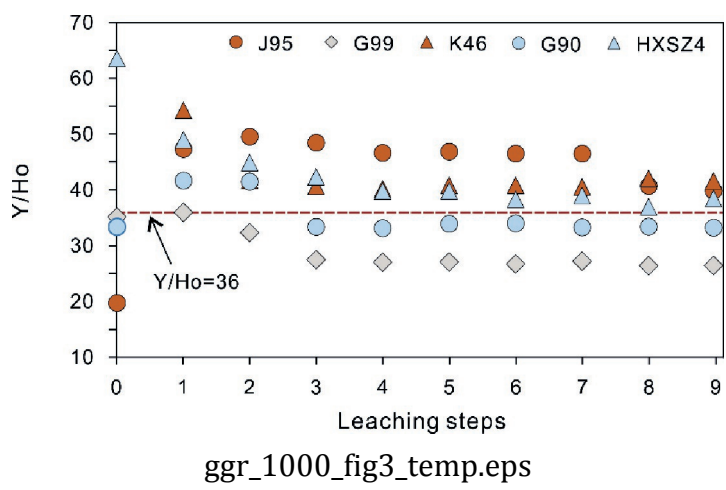
ggr_1000_fig4_temp.eps

ggr_1000_fig5_temp.eps

ggr_1000_fig6_temp.eps

ggr_1000_fig7_temp.eps